第 48 卷 第 10 期
2021 年 10 月

湖南大学学报（自然科学版）
Journal of Hunan University (Natural Sciences)

Vol. 48 No. 10
October 2021

Open Access Article

Identification of Diabetes Mellitus and High Cholesterol Based on Iris Image

Rinci Kembang Hapsari[1,2], Miswanto Miswanto[3], Riries Rulaningtyas[4*], Herry Suprajitno[3]

[1] Faculty of Sciences and Technology, Airlangga University, Surabaya, Indonesia

[2] Department of Informatics, Faculty of Electrical and Information Technology, Adhi Tama Institute of Technology, Surabaya, Indonesia

[3] Department of Mathematics, Faculty of Sciences and Technology, Airlangga University, Surabaya, Indonesia

[4] Department of Physics, Faculty of Sciences and Technology, Airlangga University, Surabaya, Indonesia

Abstract: An unhealthy lifestyle can impact body health, causing, for example, metabolic syndrome and hypercholesterolemia. Metabolic syndrome, including high blood sugar, causes diabetes mellitus (DM). Abnormal cholesterol levels cause hypercholesterolemia (HC), which contributes to various forms of cardiovascular disease (CVD). According to the WHO, DM and CVD are the main causes of death in the top ranking. Early detection of DM and HC is necessary to reduce mortality from these two diseases. This paper aims to provide an alternative for early detection of DM and HC, with a non-invasive method based on the iris image. The main contribution of this paper is to use the 3D-GLCM algorithm to detect two diseases simultaneously. The iris image processing is carried out in several stages, namely: 1) Pre-processing is done by converting the RGB image to grayscale and image improvement using the AHE method; 2) Feature extraction is carried out using the 3D-GLCM method with six statistical characteristics; 3) Classification is carried out by training and testing on Dataset I and Dataset II. The method effectiveness is compared to the number of gray levels, namely 16, 32, 64, 128, and 256. Based on the five levels of gray, the best value is shown from the number of gray levels of 256, with the value obtained. These values are sensitivity value (0.9375), specificity value (0.0208), and accuracy (0.9844). The results showed that the higher the gray level of the image database used, the higher the sensitivity and accuracy values, while the lower the gray level indicates the specificity value.

Keywords: detection, iris image, feature extraction, 3-Dimensional Gray-Level Co-Occurrence Matrix, grayscale image.

基于虹膜图像识别糖尿病和高胆固醇

摘要：不健康的生活方式会影响身体健康，导致例如代谢综合征和高胆固醇血症。代谢综合征，包括高血糖，会导致糖尿病 (DM)。胆固醇水平异常会导致高胆固醇血症 (慧聪)，从而导致各种形式的心血管疾病 (化学气相沉积)。根据世界卫生组织，DM 和化学气相沉积是排名靠前的主要死亡原因。DM 和慧聪的早期检测对于降低这两种疾病的死亡率是必要的。本文旨在通过一种基于虹膜图像的非侵入性方法，为 DM 和慧聪的早期检测提供一种替代方案。本文的主要贡献是使用 3D-GLCM 算法同时检测两种疾病。虹膜图像处理分几个阶段进行，即：1）预处理是通过将 RGB 图像转换为灰度图像并使用 AHE 方法进行图像改进；2）特征提取采用 6 个统计特征的 3D-GLCM 方法进行；3）通过对数据集 I 和数据集 II 进行训练和测试来进行分类。将方法

Received: June 26, 2021 / Revised: August 23, 2021 / Accepted: September 17, 2021 / Published: October 30, 2021

About the authors: Rinci Kembang Hapsari, Doctoral Student at the Faculty of Sciences and Technology, Airlangga University, Surabaya, Indonesia; Department of Informatics, Faculty of Electrical and Information Technology, Adhi Tama Institute of Technology, Surabaya, Indonesia; Miswanto, Department of Mathematics, Faculty of Sciences and Technology, Airlangga University, Surabaya, Indonesia; Riries Rulaningtyas, Department of Physics, Faculty of Sciences and Technology, Airlangga University, Surabaya, Indonesia; Herry Suprajitno, Department of Mathematics, Faculty of Sciences and Technology, Airlangga University, Surabaya, Indonesia

*Corresponding Author's name : Riries Rulaningtyas, E-mail : riries-r@fst.unair.ac.id.

有效性与灰度级数进行比较，即 16、32、64、128 和 256。基于五个灰度级，从 256 级灰度级数中得到最佳值，得到的值.这些值是灵敏度值 (0.9375)、特异性值 (0.0208) 和准确度 (0.9844)。结果表明，所用图像数据库的灰度级越高，灵敏度和准确度值越高，而灰度级越低表示特异性值。

关键词：检测、虹膜图像、特征提取、3 维灰度共生矩阵、灰度图像.

1. Introduction

Lifestyle refers to the characteristics of the inhabitants of a region at a certain time and place. It includes daily behavior and individual functioning in work, activity, pleasure, and diet. According to the WHO, lifestyle is 60% correlated with individual health and quality of life. Millions of people have practiced an unhealthy lifestyle. Thus, they suffer from a disease, disability, and even death. It causes metabolic disease, cardiovascular disease, hypertension, overweight, joint and bone problems, etc. This problem is caused by an unhealthy lifestyle [1].

An unhealthy lifestyle can lead to reduced physical activity and increased obesity. It can cause DM and generally occurs in almost all countries [2]. The prevalence of DM has increased very rapidly in recent years. Now, DM is a global health problem [3]. The International Diabetes Federation (IDF) stated that there were 425 million people with DM in 2017, with a projected 48% to 629 million by 2045 [26].

Lifestyle and eating habits have impacted not only DM but also cholesterol increase in the human body. Cholesterol is a fatty substance circulating in the blood, colored / yellowish and like a wax produced by the liver and is needed by the body. Cholesterol will have an important role in our body if the dose is right or normal. However, it will be dangerous for the baby's body if the cholesterol level in the blood is too much [4].

HC poses a significant threat to a person's health. Although it is not considered a disease, this condition can be a secondary disease and contribute to various forms of the disease, especially CVD [5]. The prevalence of hypercholesterolemia in the 25-34 year age group is 9.3%, and the 55-64 year age group increases with age up to 15.5% [6]. Currently, CVD is the leading cause of death globally. According to WHO, 31% of all deaths worldwide are caused by CVD disease, from 17.5 million people who die each year [7]. Early detection is necessary to reduce mortality from both causes of the condition, namely DM and HC.

Currently, the measurement of blood sugar and cholesterol levels is done by invasive methods. Blood sampling in an invasive method causes discomfort because it causes injury and pain [8]. Another method is needed, namely a non-invasive method to reduce discomfort.

In this paper, an alternative measurement is given using image processing technology. Early detection of DM and HC is done by using the iris image. In iridology, alternative disease diagnoses using the iris pattern, tissue weakness, eye color, damage, and other characteristics can show the patient's systemic health [9].

Figure 1 depicts the iris map or Iridology chart. The eye iris can be used to diagnose diseases, where each part of the body represents a representation of the area found in the iris.

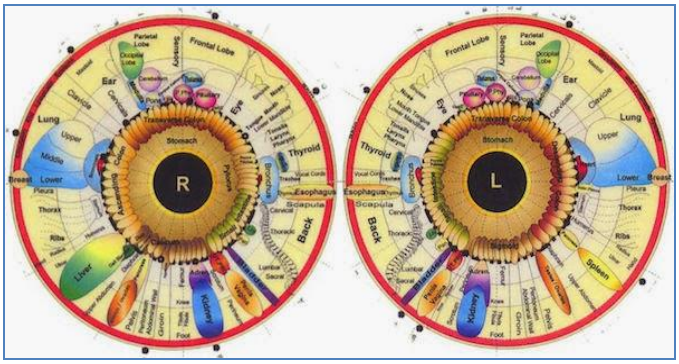

Fig. 1 Iridology map (https://www.yesmulher.com.br/mapa-iridologia/)

Traces of records relating to the intensity levels or deviations of organs caused by the disease are systematically recorded and patterned on the eye iris and surroundings. It can be used as a practical guide for diagnosing various diseases. Figure 1 shows an iridology map, a map of the eye iris, which is a detailed picture of the body's overall condition. On the right side of the body, his health condition is depicted in the right eye, and the health condition of the left body is depicted in the left iris.

There is much research related to disease diagnosis based on the image that has been done [10]-[12]. The research is related to the iris image, including detecting abnormal conditions of pancreatic Beta-cells as the cause of Diabetes Mellitus by segmentation using integral-differential operator (IDO). IDO is based on segmentation results which are used to obtain the region of interest (ROI) at 06.45-07.15 o'clock position, feature extraction with gray level co-occurrence matrix (GLCM), and adaptive neighborhood-based modified

backpropagation (ANBMP) classification. The accuracy of determining the ROI of the pancreas in this study was 87.5%, and the accuracy of detection of pancreatic damage was 83.3% [13]. This study could only detect patients with Type 1 DM.

DM can be detected by improving the image using Adaptive Median Filter [14]. Iris segmentation was done by determining the coordinates of the center of the pupil and the iris along with their radius. The segmentation results were normalized using the rubber sheet model (RSM) and classification using the Support Vector Machine (SVM) method. The result of diabetes detection accuracy was 75%. In this study, the determination of ROI was based on the iridology map and only detected one disease.

Research conducted in [15] to detect DM. In his research, image improvement was not carried out. The segmentation process used Circular Hough Transform (CHT), and the segmentation results were normalized using the RSM method. Feature extraction was carried out using the 2D Wavelet Tree method, and identification was carried out using the SVM method. The test involved 40 images of normal eyes and DM patients. The overall identification accuracy result was 87.50% [15].

DM was also detected by segmentation using CHT to determine the center coordinates and radius of the inner and outer iris [16]. As well as in the thresholding method, the researchers used the first derivative for iris edge detection. The segmentation result was normalized with RSM, and features were extracted by the wavelet transform method. This research compared six classification methods, namely Adaptive Boosting (AB), Binary Tree Model (BT), Generalized Linear (GL), Random Forest (RF), SVM, and Neural Network (NN). The used data included 200 images with 100 DM images and 100 non-DM images, with 70% of the image data used for training and 30% used for testing. The results of the accuracy of the BT method were 75.2%, RF 89.66%, AB 89.1%, SVM 88.54%, GL 62.35% and NN 67.29%.

In [5], cholesterol was detected by segmentation using the Hough Transform (HT) method, normalizing with RSM. ROI was determined at 30% of the normalized results. Cholesterol detection involved detecting arcus lipoids [5].

In [8], cholesterol was detected by segmentation using the CHT method, and RSM normalization. ROI was determined at 30% of the normalized results. Identification was carried out with OTSU threshold.

In [17], cholesterol was detected using ROI from the segmentation results according to the iridology chart. The feature extraction process comprised the Gabor Filter, color moments, mean and standard deviation. Furthermore, using the SVM method in its classification produces 95-96%.

Research on disease detection based on the eye iris has been carried out only to detect one disease or one organ abnormality. In this study, two abnormalities were detected at once, namely DM and HC. Thus, the iris is detected from the input image whether it was suffering from DM, HC, DM, and HC, or in normal condition. The feature extraction method, 3D Gray Level Co-occurrence Matrix (3D GLCM), ensures iris detection. The image data was taken from patients from the Internal Medicine Poly outpatient installation at the Airlangga University Hospital based on Passing the Ethics Review No: 111/KEP/2020 published by the Airlangga University Hospital Research Ethics Committee.

2. Materials and Methods

This section described the identification of DM and HC based on iris images using 3-Dimensional Gray-Level Co-Occurrence Matrix (3D-GLCM). The system architecture is shown in Figure 2.

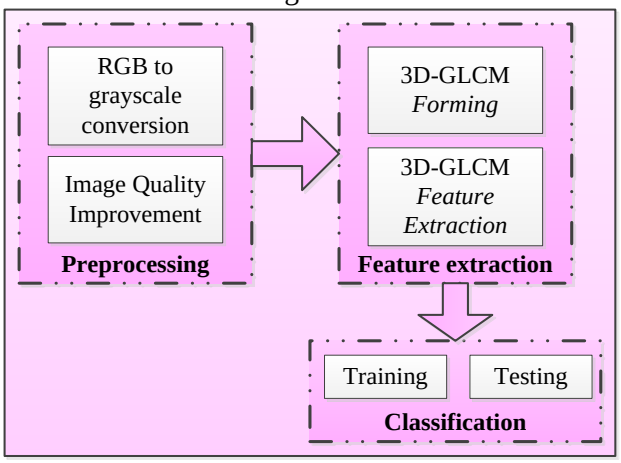

Fig. 2 Iris identification system architecture

This paper proposed a feature extraction approach using 3D-GLCM and similarity-based classification. This study consisted of three steps, namely preprocessing, feature extraction, and classification.

2.1. Dataset

The samples of iris images from one hundred patients in the outpatient department, Internal Medicine Polyclinic, Airlangga University Hospital, have been obtained samples. Where samples were taken as many as one hundred patients with specifications of 25 patients

suffering from DM, 25 patients with high cholesterol, 25 patients suffering from DM and high cholesterol, and 25 patients with normal conditions (blood sugar and cholesterol levels were on a normal scale). Before data collection, the ethics test session was conducted at the Airlangga University Hospital Research Ethics Committee with a statement that it passed the Ethics Review no: 111/KEP/2020.

The iris image captured device was used by using a 12MP iridology camera eye iriscope. The first procedure in taking the iris image is carried out on patients who are willing to participate in the study and meet the inclusion criteria that have been determined in the selection of subjects. The inclusion criteria of the subjects in this study were males or females, aged >= 20 years, who did not have cataracts, their irises were never injured, and the iris was not photographed postoperatively. Second, it was done after the patient does a blood test to check random blood sugar and cholesterol levels. The iris image was taken in the right eye and the left eye three times each.

2.2. Pre-Processing

Pre-processing is the most important part of producing a higher level of accuracy[12]. In the preprocessing step, two processes were carried out. The first process was to convert the RGB input image into a grayscale image. The second process was to improve the grayscale image using the Adaptive Histogram Equalization (AHE) method.

2.2.1. RGB to Grayscale Conversion

The RGB to Grayscale conversion process in this study used the rgb2gray() function in Matlab, where the rgb2gray function converted the RGB image to grayscale by eliminating hue and saturation information while maintaining luminosity [18].

NTSC standard conversion formula used to calculate the effective exposure of a pixel as in equation (1):

$$i = 0.2989 * red + 0.5870 * green + 0.1140 * \quad blue \quad (1)$$

2.2.2. Image Improvement with AHE Method

Adaptive Histogram Equalization (AHE) is an image processing technique that increases the contrast to obtain an image with an intensity value which will make the pixel point solid black at the darkest pixel point and each brilliant white at the brightest one [19]. In medical imaging, AHE is used for contrast enhancement techniques and produces excellent images.

In AHE, the histogram equalization process is carried out on each block (tile). The blocks (tiles) are generated by dividing the image by the size of n x n. Each block size varies in size and gives different results. Where between tiles on some pixels can overlap [20], [21]. Equation (2) is the formula for calculating the gray value using the AHE method.

$$K_o = round\left(\frac{C_i(2^k-1)}{M.N}\right) \quad (2)$$

where:
C_i - cumulative of i grayscale value of the original image;
$Round$ - rounding operation to the nearest integer;
K_0 - output value of adaptive histogram equalization;
k - number of image grayscale bits;
M - height of the image;
N - width of the image.

2.3. Feature Extraction

The feature extraction process was one of the important processes in recognizing the class of an image object, which aimed to measure the quantitative magnitude of the characteristics of each pixel. The results of this process represented the characteristics of an object that can distinguish object classes well. In this study, the feature extraction process used was the 3D-GLCM method.

3D-GLCM Forming, Texture analysis using 3D-GLCM considered the relationship between three pixels called reference and two neighboring pixels. Figure 3 shows the pixel relations in spatial space and the structure of 3D-GLCM where R is the reference pixel, N1 is the first neighboring pixel, N2 is the second neighbor pixel, i is the number of rows, j is the number of columns, and k is the number of layers in 3D-GLCM.

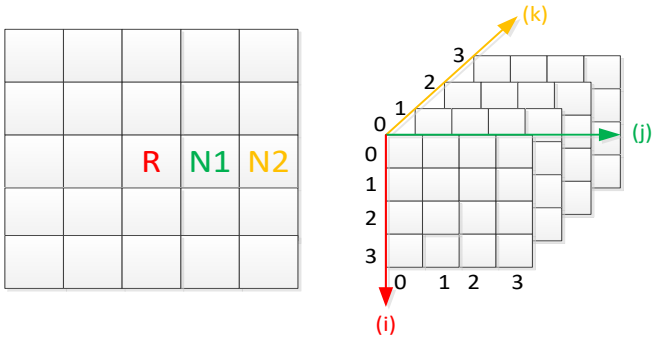

(a) (b)

Fig. 3 (a) Spatial pixel relations; (b) 3D-GLCM structure

Figure 4 shows the steps in the formation of the 3D-GLCM matrix where iris image had been converted into a grayscale image, and image improvements had been made using AHE.

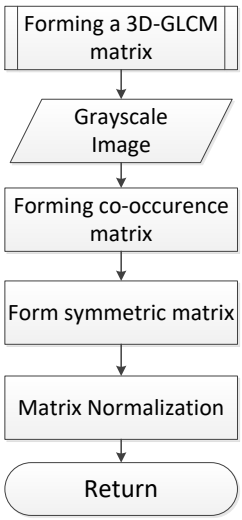

Fig. 4 3D-GLCM matrix formation flow

Figure 5 illustrates how to form a co-occurrence matrix at a distance of d=1 pixel and direction =0^0 with a 7x7 grayscale image and with 4 gray values (0, 1, 2, and 3).

2	0	1	1	2	0	2
1	0	2	1	0	2	3
3	2	0	3	2	1	0
0	1	0	2	3	1	2
0	3	2	0	1	2	0
1	1	0	3	2	0	2
1	2	3	2	1	0	2

(a)

Second Neighbor's Gray Value (k=0)	First Neighbor's Gray Value (j)			
Reference Gray Value (i)	0	1	2	3
0	0	1	0	0
1	0	1	2	0
2	0	3	0	0
3	0	0	3	0

(b)

Second Neighbor's Gray Value (k=1)	First Neighbor's Gray Value (j)			
Reference Gray Value (i)	0	1	2	3
0	0	1	1	0
1	0	0	0	0
2	2	0	0	1
3	0	0	2	0

(c)

Second Neighbor's Gray Value (k=2)	First Neighbor's Gray Value (j)			
Reference Gray Value (i)	0	1	2	3
0	0	1	0	2
1	4	1	0	0
2	2	0	0	1
3	0	1	0	0

(d)

Second Neighbor's Gray Value (k=2)	First Neighbor's Gray Value (j)			
Reference Gray Value (i)	0	1	2	3
0	0	0	0	0
1	1	0	1	0
2	1	0	0	0
3	0	0	0	0

(e)

Fig. 5 (a) 7x7 grayscale image with 4 gray values; (b) co-occurrence matrix 4x4 layer k = 0; (c) co-occurrence matrix 4x4 layer k = 1; (d) co-occurrence matrix 4x4 layer k = 2; (e) co-occurrence matrix 4x4 layer k = 3

2.3.1. 3D-GLCM Feature Extraction

After being formed, the 3D-GLCM matrix was at a distance of d and in all possible directions. The next step was to calculate the statistical characteristics of all the 3D-GLCM matrices that were formed. In this study, six statistical characteristics were used, namely:

1) Max Probability

Max Probability shows the size of the response strength of the co-occurrence matrix with a range of values [0,1], which is 0 to 1 [22]. The method of calculating the max probability is shown in equation (3):

$$Max\ probability = max(p_{ij}) \quad (3)$$

where:
i = i^{th} row in 3D-GLCM;
j = j^{th} column in 3D-GLCM;
k = k^{th} layer in 3D-GLCM;
p_{ijk} = ijk-element in the normalized matrix.

2) Entropy

Entropy shows a measure of the irregularity of the intensity distribution of an image in the co-occurrence matrix. Entropy = 0, if all elements of p_{ijk} are 0, and will be maximum when all elements of p_{ijk} are equal. The maximum value is $2log_2 K$ [22]. The method of calculating entropy is shown in equation (4) below:

$$Entropi = -\sum_{i=1}^{Q}\sum_{j=1}^{Q}\sum_{k=1}^{Q} p_{ijk}(\log_2 p_{ijk}) \quad (4)$$

where:
Q = matrix size;
i = i^{th} row in 3D-GLCM;
j = j^{th} column in 3D-GLCM;
k = k^{th} layer in 3D-GLCM;
p_{ijk} = ijk^{th} element in the normalized matrix.

It is assumed that the value of entropy = 0 if all elements of p_{ijk} are 0.

3) Energy

Energy is a feature to measure the concentration of intensity pairs in the co-occurrence matrix with a value range of [0,1], which is 0 to 1 [22]. The energy value will increase if the pixel pairs that meet the requirements of the co-occurrence intensity matrix are concentrated in several coordinates and decrease if they are spread out. The method of calculating energy is in equation (5).

$$Energi = \sum_{i=1}^{Q}\sum_{j=1}^{Q}\sum_{k=1}^{Q} p_{ijk}^2 \quad (5)$$

where:
Q - matrix size
i = i^{th} row in 3D-GLCM;

j = j[th] column in 3D-GLCM;
k = k[th] layer in 3D-GLCM;
p_{ijk} = ijk[th] element in the normalized matrix.

4) Correlation

This feature shows the level of correlation between pixels in an image with a value range of 1 to -1. This measure is undefined if one of the standard deviations is 0 [25]. The way of calculating the correlation is shown in equation (6) as follows:

$$Korelasi = \sum_{i=1}^{Q}\sum_{j=1}^{Q}\sum_{k=1}^{Q} p_{ijk}\frac{(i-\mu_x)(j-\mu_y)(k-\mu_z)}{\sigma_x\sigma_y\sigma_z} \quad (6)$$

where:
Q = matrix size;
i = i[th] row in 3D-GLCM;
j = j[th] column in 3D-GLCM;
k = k[th] layer in 3D-GLCM;
p_{ijk} = ijk[th] element in the normalized matrix;
μ_x = average of the i[th] pixel values;
μ_y = average of the j[th] pixel values;
μ_z = average of the k[th] pixel values;
σ_x = i[th] pixel standard deviation;
σ_y = j[th] pixel standard deviation;
σ_z = k[th] pixel standard deviation.

5) Contrast

Contrast is a feature used to measure the strength of the difference in intensity in the image with a value range of 0 (when the co-occurrence matrix is constant) to $(Q-1)^2$ [22]. The contrast value increases if the variation in image intensity is high and decreases when the variation is low. The equation used to measure the contrast of an image is shown in equation (6) below:

$$Contrast = \sum_{i=1}^{Q}\sum_{j=1}^{Q}\sum_{k=1}^{Q} p_{ijk}\left[(i-j)^2+(i-k)^2+(j-k)^2\right] \quad (6)$$

where:
Q - matrix size;
i - i[th] row in 3D-GLCM;
j - j[th] column in 3D-GLCM;
k - k[th] layer in 3D-GLCM;
p_{ijk} - ijk[th] element in the normalized matrix.

6) Homogeneity

Homogeneity is used to measure the spatial proximity of the distribution in the diagonal elements of the co-occurrence matrix—the variation of image intensity with a value range of 0 to 1. The maximum is achieved when the co-occurrence matrix is in the form of a diagonal matrix[22]. The homogeneity value increases when the intensity variation in the image decreases. The method of calculating homogeneity is shown in equation (7) below:

$$Homogenitas = \sum_{i=1}^{Q}\sum_{j=1}^{Q}\sum_{k=1}^{Q}\frac{p_{ijk}}{\left[(i-j)^2+(i-k)^2+(j-k)^2\right]} \quad (7)$$

where:
Q - matrix size;
i = i[th] row in 3D-GLCM;
j = j[th] column in 3D-GLCM;
k = k[th] layer in 3D-GLCM;
p_{ijk} = ijk[th] element in the normalized matrix.

The statistical feature extraction process results are used as input data in training to identify input patterns and pairs of output patterns (Figure 6).

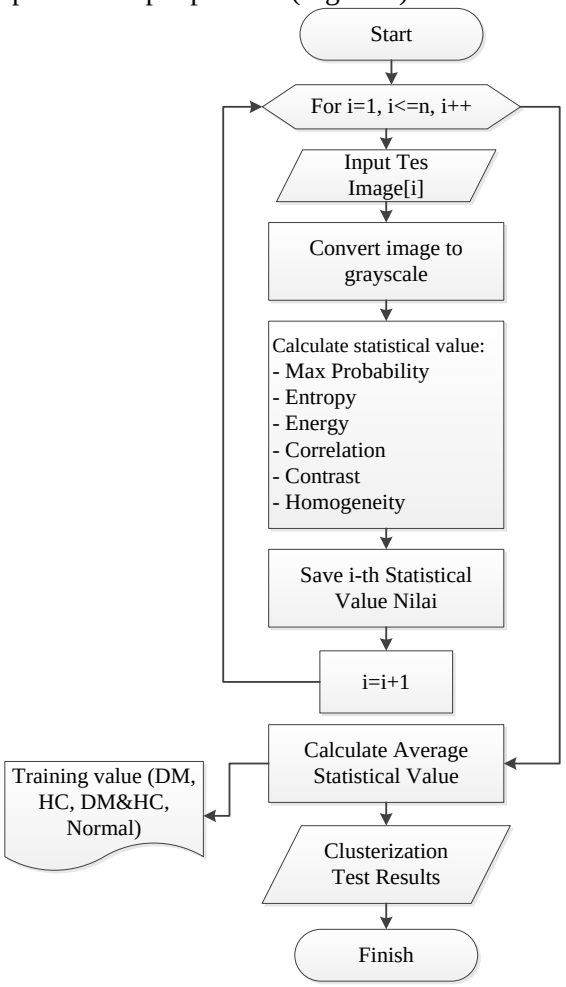

Fig. 6 Steps of the training process

2.4. Classification

The classification step in this research was divided into two processes, namely the learning and testing process. Both processes have referred to the results of statistical feature extraction calculations. The statistical feature extraction parameters used are maximum probability (max probability), entropy, energy, correlation, contrast, and homogeneity.

The training process in this study was based on the calculation results of statistical feature extraction using 3D-GLCM. This value becomes input data in the learning process. Figure 6 shows the flow of the learning process.

2.4.1. Testing

The testing process was done by measuring the distance of each test image to the group value parameters resulting from the training process. The distance here

was used to determine the degree of similarity or dissimilarity of two feature vectors. The steps of the training process are shown in Figure 7. Distance measurement was used by the Euclidean distance (ED) method.

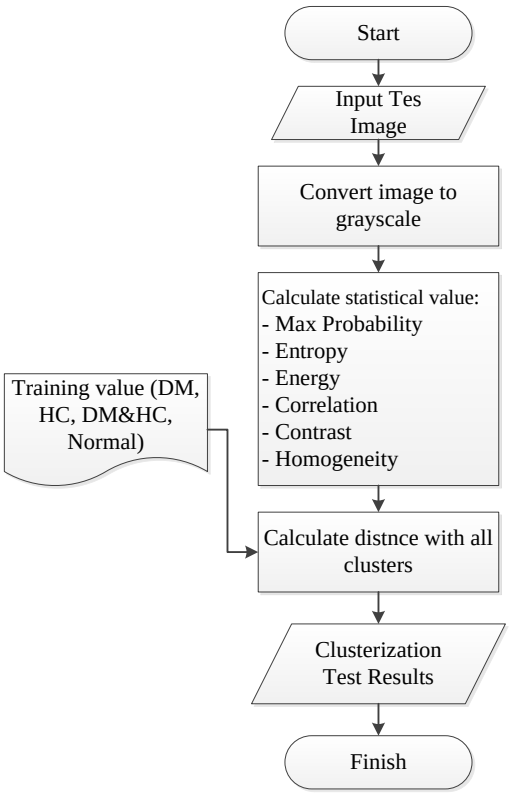

Fig. 7 Steps of the testing process

ED is a metric used to measure the similarity of two vectors. ED calculates the square root of the difference of two vectors, and the formula is shown in equation (8) [23]

$$d_{ij} = \sqrt[2]{\sum_{k=1}^{n}(x_{ik} - x_{jk})^2} \quad (8)$$

where:
d_{ij} = Euclidean distance between *i and j;*
i = ith data;
j = j^{th} data.

3. Results and Discussion

This study tested the performance of the 3D-GLCM method on two iris datasets. Dataset I contained 100 images of the right iris for learning and testing. Dataset II contained 100 images of the left iris for learning and for testing too.

At the testing stage, the cross-validation (CV) technique has been carried out. The dataset is separated into two subsets, namely learning process data and testing process data. Tests carried out on the dataset have used 80 images as learning data, and 20 images have been used for testing so that in this study, a 5-fold CV has been used.

Evaluation of the classification results was done by using the confusion matrix method. The confusion matrix has provided details of misclassification. The predicted class was shown at the top of the matrix, and the observed class is on the left. Each cell contained a number representing the actual number of cases of the class observed by the model for a given prediction class, shown in Figure 8 [24].

		Predicted Class	
		YES	NO
Observed Class	YES	a (True Positive – TP)	b (False Negative – FN)
	NO	c (False Positive – FP)	d (True Negative – TN)

Fig. 8 Confusion matrix for 2-Class

This study was divided into four classes: DM class, HC class, DM and HC class, and normal class. In the multi-class classification, sensitivity, specificity, and accuracy were calculated through the average sensitivity, specificity, and accuracy for each class, where the calculation formula is shown in equations (9) to (11).

$$Sensitivity = \frac{\sum_{i=1}^{k} TP_i}{\sum_{i=1}^{k}(TP_i + FN_i)} \quad (9)$$

$$Specificity = \frac{\sum_{i=1}^{k} TN_i}{\sum_{i=1}^{k}(FP_i + TN_i)} \quad (10)$$

$$Accuracy = \frac{\frac{\sum_{i=1}^{k}(TP_i + TN_i)}{\sum_{i=1}^{k}(TP_i + TN_i + FP_i + FN_i)}}{k} * 100\% \quad (11)$$

where:
k - number of classes;
TP_i - true positive for the ith class;
TN_i - true negative for the ith class;
FN_i - false negative for the ith class;
FP_i - false positive for the ith class.

The number of positive data classified correctly by the system is called True positive. The number of negative data that are classified correctly by the system is called True negative. The number of positive data but reclassified incorrectly by the system is called False Negative. The number of negative data classified correctly by the system is called a false negative [25].

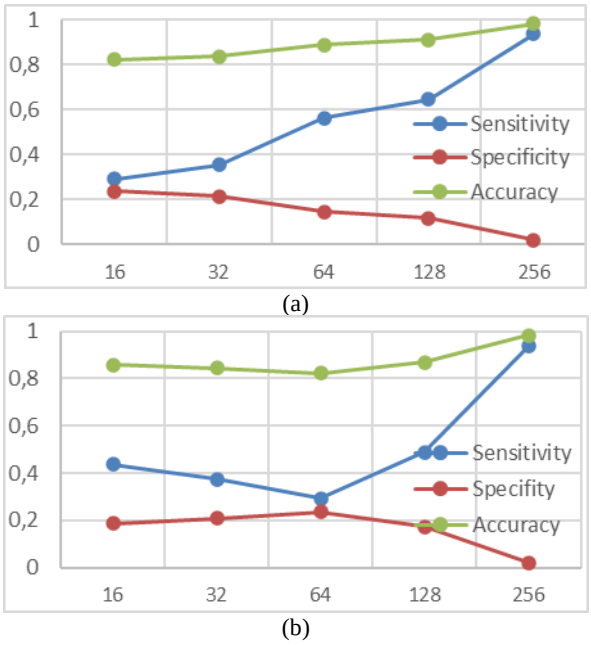

Fig. 9 Sensitivity, specificity and accuracy values: a) Test results on Dataset I; b) Test results on Dataset II

The obtained test results were used to calculate the sensitivity, specification, and accuracy.

Figure 9a shows the test results on Dataset I, and Figure 9b shows the test results on Dataset II. The test results were carried out by measuring the value of sensitivity, specificity, and accuracy to differences in the image gray level.

It was done by comparing four gray levels; they are the gray level of the 4-bit gray-level which consists of 16 gray levels; the 5-bits gray-level, which consists of 32 gray levels; the 6-bits, which consist of 64 gray levels; and the 7 bits and 8 bits which consists of 256 gray levels.

4. Conclusions

This paper proposes to identify two disease disorders at once in a 3D-GLCM algorithm where the output is the identification of early detection in one of the four possible clusters, namely DM, HC, DM, and HC or normal.

In this paper, identification with 3D-GLCM has been carried out by comparing the gray levels of 16, 32, 64, and 256. The test results show that the more gray levels contained in the image, the higher the sensitivity and accuracy values. While the specificity value is getting smaller, the 3D-GLCM method can get a good recognition rate.

The limitation of this study is the small number of datasets. However, this can be solved by using the cross-validation method. Another weakness is in the iris image that is generated during data retrieval. Where if the eye shape of the respondent is small/slanted, the iris taken will be covered by the eyelids, and if the respondent has thick eyelashes, it causes noise in the iris in the form of eyelashes. The existence of this weakness affects the value of accuracy, specifications, and sensitivity.

Therefore, to test the performance of the algorithm in future research, it is necessary to pay attention to the collection of iris data that is free from eyelid and eyelash noise.

Acknowledgment

We would like to thank the Outpatient Installation, Internal Medicine Polyclinic, Airlangga University hospital that provided the researchers with a support in collecting patients' iris image data.

References

[1] FARHUD D. D. Impact of Lifestyle on Health. *Iranian Journal of Public Health*, 2015, 44(11): 1442–1444.

[2] SHAW J. E., SICREE R. A., and ZIMMET P. Z. Global estimates of the prevalence of diabetes for 2010 and 2030. *Diabetes Research and Clinical Practice*, 2010, 87(1): 4–14.

[3] GUARIGUATA L., WHITING D. R., HAMBLETON I., et al. Global estimates of diabetes prevalence for 2013 and projections for 2035. *Diabetes Research and Clinical Practice*, 2014, 103(2): 137–149.

[4] ANGGRAINI D. I. and NABILLAH L. F. Activity Test of Suji Leaf Extract (Dracaena angustifolia Roxb.) on in vitro cholesterol lowering. *Jurnal Kimia Sains dan Aplikasi*, 2018, 21(2): 54.

[5] RAMLEE R. A. and RANJIT S. Using iris recognition algorithm, detecting cholesterol presence. *Proceedings of the 2009 International Conference on Information Management and Engineering, ICIME 2009*: 714–717, 2009.

[6] ARIANTARI N. P., YOWANI S. C., and SWASTINI D. Uji Aktivitas Penurunan Kolesterol Produk Madu Herbal yang Beredar di Pasaran pada Tikus Putih Diet Lemak Tinggi. *Jurnal Kimia* 2010, 4(1): 15–19.

[7] WHO. Cardiovascular diseases. *World Health Organization: Geneva, Switzerland*, 2017. https://www.who.int/news-room/fact-sheets/detail/cardiovascular-diseases-(cvds).

[8] RAMLEE R. A., AZIZ K. A., RANJIT S., and ESRO M. Automated Detecting Arcus senilis, symptom for Cholesterol Presence using Iris Recognition Algorithm. *Journal of Telecommunication, Electronic and Computer Engineering*, 2011, 3(2): 29–39.

[9] HARRIS P. E., COOPER K. L., RELTON C., and THOMAS K. J. Prevalence of complementary and alternative medicine (CAM) use by the general population: A systematic review and update. *International Journal of Clinical Practice*, 2012, 66(10): 924–939.

[10] JILANI SAUDAGAR A. K. Biomedical Image Compression Techniques for Clinical Image Processing. *International Journal of Online and Biomedical Engineering*, 2020, 16(12): 133–154.

[11] SAMREEN A., TAHA A. M., REDDY Y. V., and SATHISH P. Brain Tumor Detection by Using Convolution Neural Network. *International Journal of Online and Biomedical Engineering*, 2020, 16(13): 58–69.
[12] RAJESH P., MURUGAN A., MURUGANANTHAM B., and GANESH KUMAR S. Lung Cancer Diagnosis and Treatment Using AI and Mobile Applications. *International Journal of Interactive Mobile Technologies*, 2020, 14(17): 189–203.
[13] LESMANA I. P. D., PURNAMA I. K. E., and PURNOMO H. P. Abnormal Condition Detection of Pancreatic Beta-Cells as the Cause of Diabetes Mellitus Based on Iris Image. *Proceedings of the International Conference on Instrumentation, Communication, Information Technology and Biomedical Engineering*, 2011, November: 4–9.
[14] PERGAD N. and MORE S. B. Detection of diabetic presence from iris by using support vector machine. *International Journal of Engineering Sciences and Research*, 2015, 4(7): 562–565.
[15] BANSAL A., AGARWAL R., and SHARMA R. K. Determining diabetes using iris recognition system. *International Journal of Diabetes in Developing Countries*, 2015, 35(4): 432–438.
[16] SAMANT P. and AGARWAL R. Diagnosis of Diabetes Using Computer Methods: Soft Computing Methods for Diabetes Detection Using Iris. *Internation Journal of Medical, Health, Biomedical, Bioengineering and Pharmaceutical Engineering*, 2017, 200(2): 57–62.
[17] PRASAD J., PATEL D., and JADHAV M. Iris Based Medical Analysis by Geometric Deformation Features. *International Research Journal of Engineering and Technology (IRJET)*, 2016, 03(04): 2553–2556.
[18] MATLAB, rgb2gray. 2021. https://www.mathworks.com/help/matlab/ref/rgb2gray.html#description.
[19] ZHU Y. and HUANG C. An Adaptive Histogram Equalization Algorithm on the Gray Level Image. *Physics Procedia*, 2012, 25: 601–608.
[20] GUPTA S. and KAUR Y. Review of Different Local and Global Contrast Enhancement Techniques for a Digital Image. *International Journal of Computer Applications*, 2014, 100(18): 18–23.
[21] HAPSARI R. K., UTOYO M. I., RULANINGTYAS R., and SUPRAJITNO H. Comparison of Histogram Based Image Enhancement Methods on Iris Images. *Journal of Physics: Conference Series*, 2020, 1569(2), article ID 022002.
[22] GONZALEZ R. C. and WOODS R. E. *Digital Image Processing*. Third Edition, Pearson Prentice Hall, 2008.
[23] AULIA S., SUSANTO E., and ASTUTI D. Comparison of Different Classifiers for Drowsiness Detection Based on Facial Expression Recognition. *Journal of Hunan University Natural SciencesNatural Sciences*, 2021, 48(1).
[24] GORUNESCU F. *Data Mining Concepts, Models and Techniques*, 12th ed. Springer, 2011.
[25] HAPSARI R. K., UTOYO M. I., RULANINGTYAS,R. and SUPRAJITNO H. Iris segmentation using Hough Transform method and Fuzzy C-Means method. *Journal of Physics: Conference Series*, 2020, 1477, article ID 022037.
[26] International Diabetes Federation. (2017) IDF Diabetes Atlas, 8th edition. https://diabetesatlas.org/upload/resources/previous/files/8/IDF_DA_8e-EN-final.pdf

参考文:

[1] FARHUD D. D. 生活方式对健康的影响。伊朗公共卫生杂志，2015，44(11)：1442–1444。
[2] SHAW J. E.、SICREE R. A. 和 ZIMMET P. Z. 2010 年和 2030 年糖尿病患病率的全球估计。糖尿病研究和临床实践，2010，87(1)：4-14。
[3] GUARIGUATA L., WHITING D. R., HAMBLETON I.，等。2013 年全球糖尿病患病率估计和 2035 年预测。糖尿病研究和临床实践，2014，103(2)：137–149。
[4] ANGGRAINI D. I. 和 NABILLAH L. F. 须吉叶提取物(龙血树罗克斯.) 对体外降低胆固醇的活性测试。科学与应用化学杂志,2018, 21(2): 54。
[5] RAMLEE R. A. 和 RANJIT S. 使用虹膜识别算法，检测胆固醇的存在。2009 年国际信息管理与工程会议论文集，ICIME 2009：714–717，2009。
[6] ARIANTARI N. P.、YOWANI S. C. 和 SWASTINI D. 市场上草本蜂蜜产品对高脂肪饮食白鼠的胆固醇降低活性测试。化学杂志，2010, 4(1): 15–19。
[7] 世界卫生组织。心血管疾病。世界卫生组织：瑞士日内瓦，2017。https://www.who.int/news-room/fact-sheets/detail/cardiovascular-diseases-(cvds)。
[8] RAMLEE R. A.、AZIZ K. A.、RANJIT S. 和 ESRO M. 使用虹膜识别算法自动检测老年弧菌，胆固醇存在的症状。电信，电子与计算机工程杂志，2011，3（2）：29-39。
[9] HARRIS P. E.、COOPER K. L.、RELTON C. 和 THOMAS K. J. 一般人群使用补充和替代医学 (摄像头) 的流行率：系统评价和更新。国际临床实践杂志，2012，66（10）：924-939。
[10] JILANI SAUDAGAR A. K. 用于临床图像处理的生物医学图像压缩技术。国际在线与生物医学工程杂志，2020，16（12）：133–154。

[11] SAMREEN A.、TAHA A. M.、REDDY Y. V. 和 SATHISH P. 使用卷积神经网络进行脑肿瘤检测。国际在线与生物医学工程杂志，2020，16（13）：58-69。

[12] RAJESH P.、MURUGAN A.、MURUGANANTHAM B. 和 GANESH KUMAR S. 使用人工智能和移动应用程序进行肺癌诊断和治疗。国际交互式移动技术杂志，2020，14(17)：189–203。

[13] LESMANA I. P. D.、PURNAMA I. K. E. 和 PURNOMO H. P. 基于虹膜图像的胰腺 β 细胞异常状况检测作为糖尿病的原因。仪器、通信、信息技术和生物医学工程国际会议论文集，2011，11 月：4-9。

[14] PERGAD N. 和 MORE S. B. 通过使用支持向量机从虹膜检测糖尿病患者。国际工程科学与研究杂志，2015，4(7)：562–565。

[15] BANSAL A.、AGARWAL R. 和 SHARMA R. K. 使用虹膜识别系统确定糖尿病。国际发展中国家糖尿病杂志，2015，35(4)：432–438。

[16] SAMANT P. 和 AGARWAL R. 使用计算机方法诊断糖尿病：使用虹膜检测糖尿病的软计算方法。国际医学、健康、生物医学、生物工程和制药工程杂志，2017，200(2)：57–62。

[17] PRASAD J.、PATEL D. 和 JADHAV M. 基于几何变形特征的虹膜医学分析。国际工程技术研究杂志 (射流), 2016, 03(04): 2553–2556。

[18] MATLAB，rgb2 灰色的，2021。https://www.mathworks.com/help/matlab/ref/rgb2gray.html#description。

[19] ZHU Y. 和 HUANG C. 灰度图像上的自适应直方图均衡化算法。物理学报，2012，25：601-608。

[20] GUPTA S. 和 KAUR Y. 数字图像不同局部和全局对比度增强技术的回顾。国际计算机应用杂志，2014，100(18)：18-23。

[21] HAPSARI R. K.、UTOYO M. I.、RULANINGTYAS R. 和 SUPRAJITNO H. 基于直方图的虹膜图像图像增强方法的比较。 物理学杂志：会议系列，2020, 1569(2), 文章 ID 022002。

[22] GONZALEZ R. C. 和 WOODS R. E. 数字图像处理。第三版，皮尔逊普伦蒂斯大厅，2008。

[23] AULIA S.、SUSANTO E. 和 ASTUTI D. 基于面部表情识别的睡意检测不同分类器的比较。湖南大学自然科学学报自然科学, 2021, 48(1).

[24] GORUNESCU F. 数据挖掘概念、模型和技术，第 12 版。斯普林格，2011。

[25] HAPSARI R. K., UTOYO M. I., RULANINGTYAS, R. 和 SUPRAJITNO H. 使用 霍夫变换方法和模糊 C 均值方法。物理学杂志：会议系列，2020，1477，文章 ID 022037。

[26] 国际糖尿病联合会。(2017) 以色列国防军糖尿病地图集，第 8 版。https://diabetesatlas.org/upload/resources/previous/files/8/IDF_DA_8e-EN-final.pdf